nature microbiology

SUPPLEMENTARY INFORMATION

VOLUME: 2 | ARTICLE NUMBER: 17062

In the format provided by the authors and unedited.

Structural basis for λN-dependent processive transcription antitermination

Nelly Said[1], Ferdinand Krupp[2,†], Ekaterina Anedchenko[1,†,‡], Karine F. Santos[1,#], Olexandr Dybkov[3], Yong-Heng Huang[1], Chung-Tien Lee[4,6], Bernhard Loll[1], Elmar Behrmann[2,‖], Jörg Bürger[2,5], Thorsten Mielke[5], Justus Loerke[2], Henning Urlaub[4,6], Christian M. T. Spahn[2], Gert Weber[1,§], Markus C. Wahl[1,7,*]

[1] Freie Universität Berlin, Laboratory of Structural Biochemistry, Takustraße 6, D-14195 Berlin, Germany

[2] Medizinische Physik und Biophysik, Charité – Universitätsmedizin Berlin, Charitéplatz 1, D-10117 Berlin, Germany

[3] Max Planck Institut für biophysikalische Chemie, Department of Cellular Biochemistry, Am Fassberg 11, D-37077 Göttingen, Germany

[4] Max Planck Institut für biophysikalische Chemie, Bioanalytical Mass Spectrometry, Am Fassberg 11, D-37077 Göttingen, Germany

[5] Max-Planck-Institut für Molekulare Genetik, Microscopy and Cryo-Electron Microscopy Group, Ihnestraße 63-73, D14195 Berlin, Germany

[6] Universitätsmedizin Göttingen, Institut für Klinische Chemie, Bioanalytik, Robert-Koch-Straße 40, D-35075 Göttingen, Germany

[7] Helmholtz-Zentrum Berlin für Materialien und Energie, Macromolecular Crystallography, Albert-Einstein-Straße 15, D-12489 Berlin, Germany

[†] These authors contributed equally to this work.

[‡] Present address: Humboldt-Universität zu Berlin, Molecular Cell Biology, Philippstr. 13, D-10099 Berlin, Germany

[#] Present address: moloX GmbH, Takustraße 6, D-14195 Berlin, Germany

[‖] Present address: Research Group Structural Dynamics of Proteins, Center of Advanced European Studies and Research (Caesar), Ludwig-Erhard-Allee 2, D-53175 Bonn, Germany

[§] Present address: Ernst-Moritz-Arndt-Universität Greifswald, Molekulare Strukturbiologie, Felix-Hausdorff-Str. 4, D-17487 Greifswald, Germany

[*] Correspondence to: mwahl@zedat.fu-berlin.de

Supplementary Discussion

Co-transcriptional TAC assembly. Our results delineate possible steps of TAC formation during transcription elongation. NusA accompanies RNAP during elongation[1] and would thus allow early docking of λN. Initial docking might capitalize on the interaction of λN residues 34-47 with the NusA AR1 domain, which has repeatedly been observed[2-5]. Presence of a minor complex, in which λN^{34-47} interacts with the NusA AR1 domain, is also seen in our present cross-linking analyses (Supplementary Tables 2 and 3). Previous assays, which showed that the NusA AR1 domain is dispensable for antitermination[3,6], may not have been sensitive enough to reveal a beneficial, albeit not essential, role of NusA AR1 in TAC assembly. λN and NusA might then concomitantly recognize *nut* RNA *via boxB* and the *boxA-boxB* spacer, as NusA is activated for RNA binding by RNAP αCTD-AR2 and/or λN-AR1 contacts[7,8]. As NusA binding to a λN-*nut* RNP depends on NusA-RNA contacts[9], *boxB* binding to λN might induce conformational changes in neighboring λN regions to counteract the initial λN^{34-47}-AR1 interaction, initiating repositioning of λN on NusA as suggested previously[6]. Indeed, in the absence of *nut* RNA, where λN might be trapped on AR1, NusA inhibits λN function[10]. Subsequent entry of the NusB-NusE heterodimer would then be facilitated by concomitant contacts to *boxA*, NusA and λN, which are not stable individually, leading to accommodation of λN^{47-52} in the NusA-NusE cavity. NusG might join the complex independently or aided by weak NusG CTD-NusE[11] and/or NusG NTD-NusA interactions[12].

Supplementary Figures

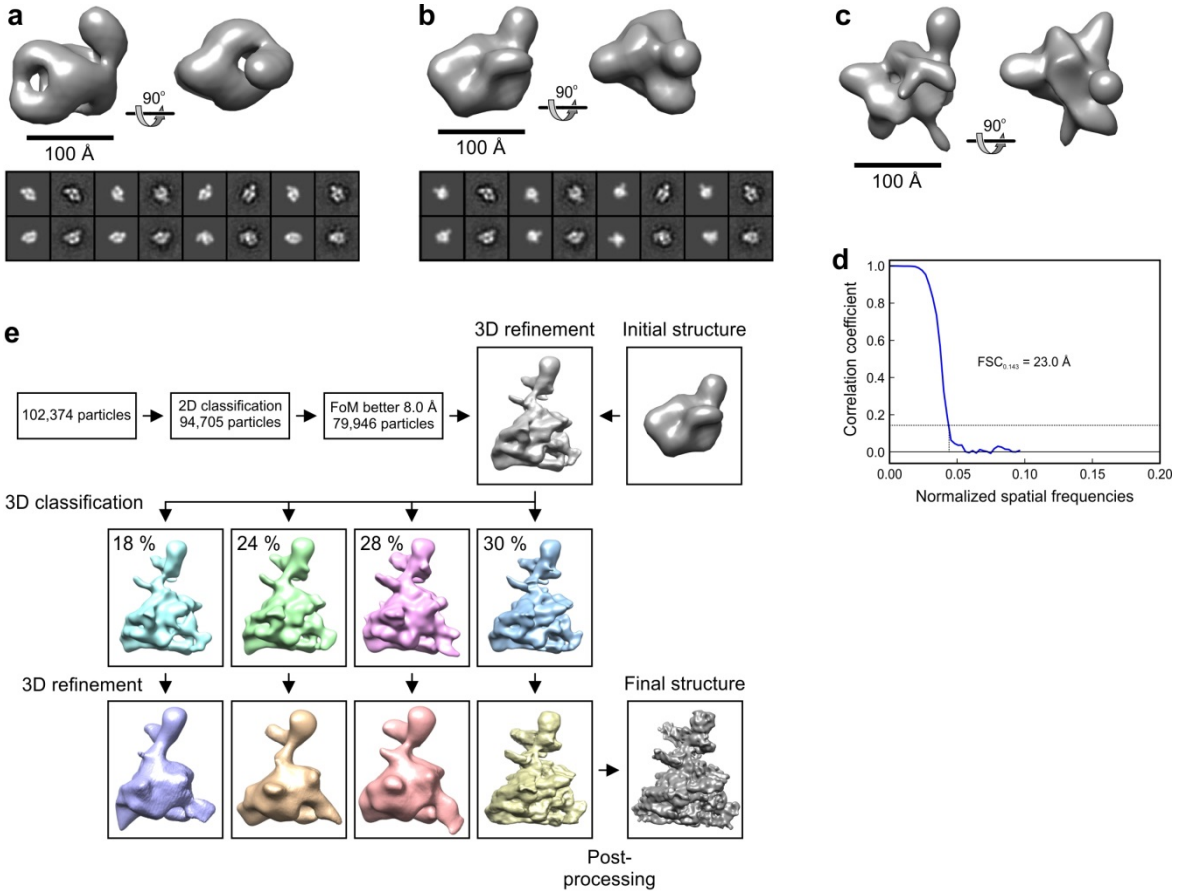

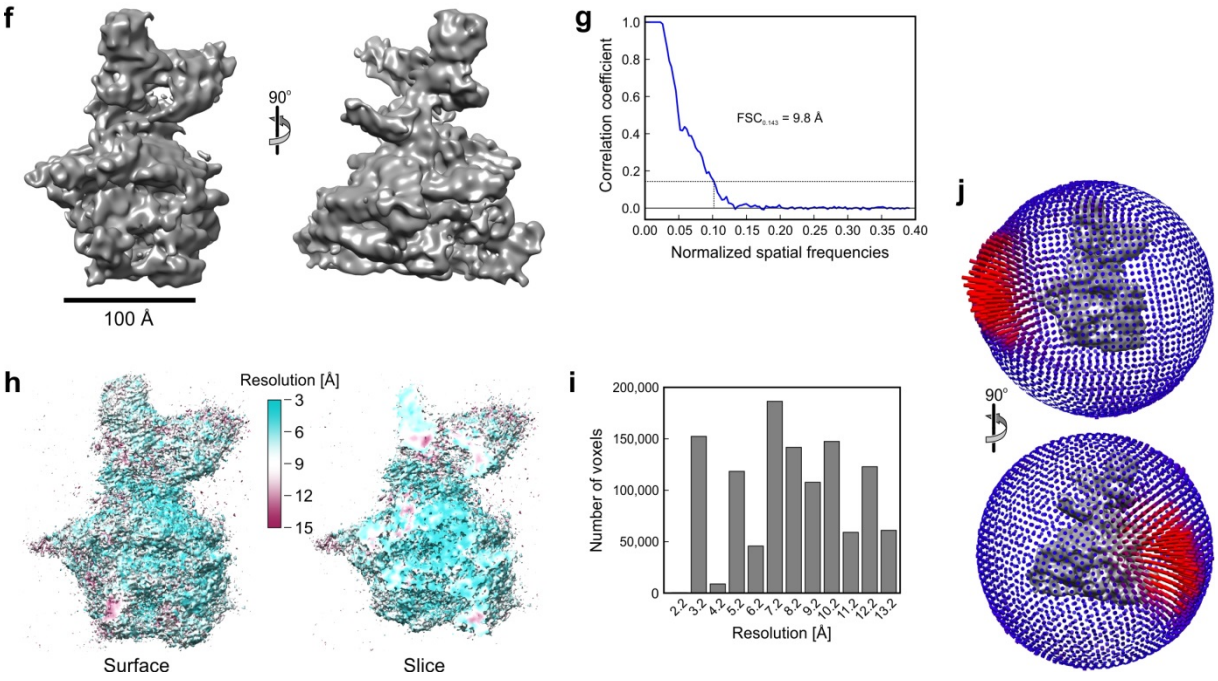

Supplementary Figure 1. EM analysis of the TAC. a, Top, orthogonal views of the initial map based on negative stain data. Bottom, comparison of re-projections of the map (left) and class averages (right). **b**, Top, orthogonal views of the map obtained after template matching of all particle images against the initial model in (**a**). Bottom, comparison of re-projections of the map (left) and class averages (right). **c**, Orthogonal views of the initial cryo-EM map. **d**, Fourier shell correlation (FSC) indicating a resolution of 23.0 Å for the map in (**c**) according to the $FSC_{0.143}$ criterion. **e**, 3D sorting of the large cryo-EM data set. FoM, Figure of Merit. 3D classification separated the data set into four classes, one of which (right) showed high-resolution features. **f**, Orthogonal views of the final cryo-EM map. **g**, FSC indicating an overall resolution of 9.8 Å based on the $FSC_{0.143}$ criterion. **h**, Unfiltered map colored according to local resolution. Left, surface view. Right, cross section view. **i**, ResMap analysis indicated higher local resolution than according to the $FSC_{0.143}$ criterion, with a large portion of voxels containing signal better than 9 Å resolution. **j**, Visualization of the distribution of Euler angles associated with the particle images.

Original Scans, Figure 2

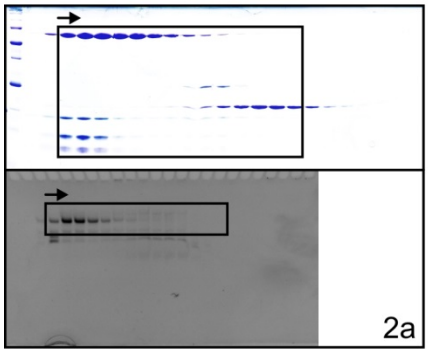

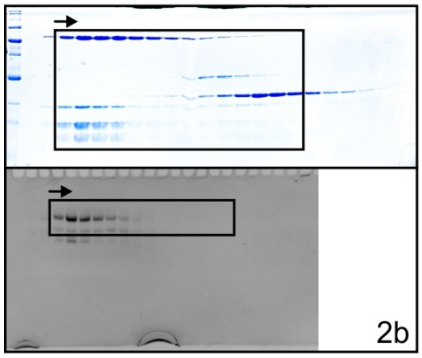

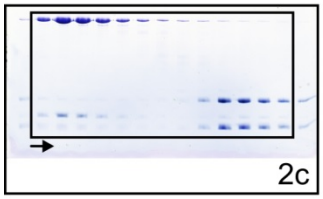

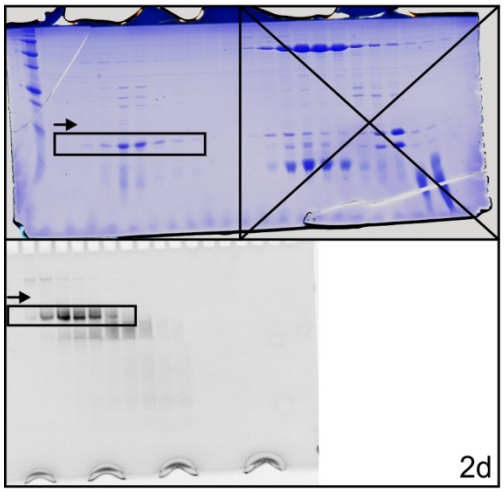

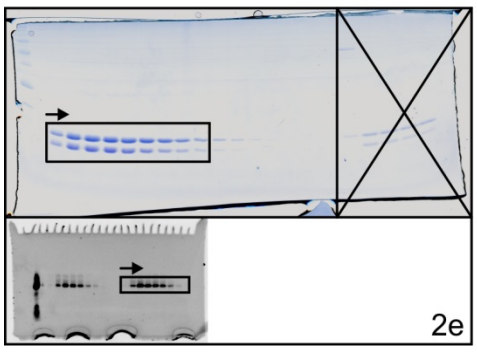

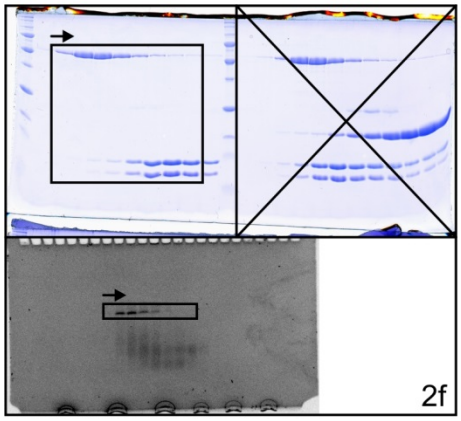

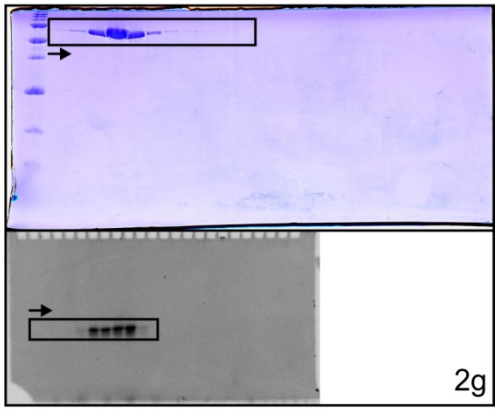

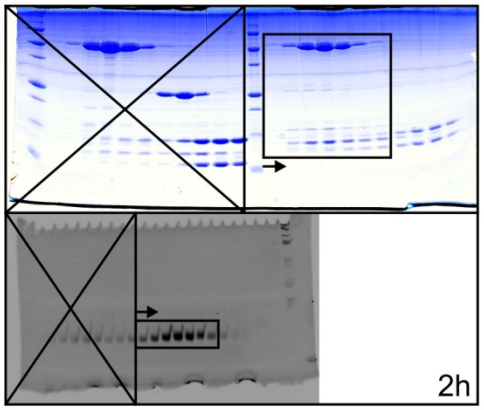

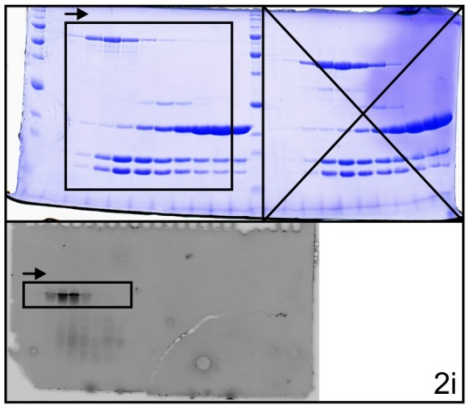

73

Original Scans, Figure 2

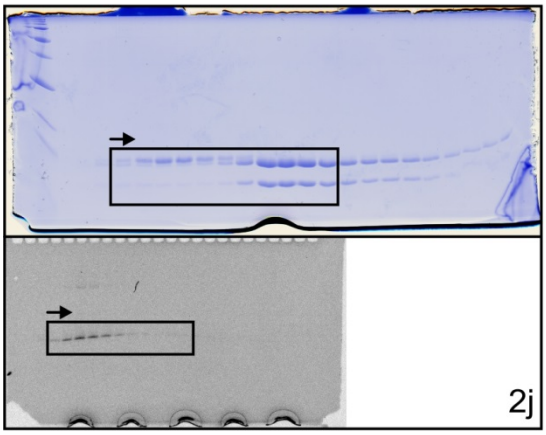

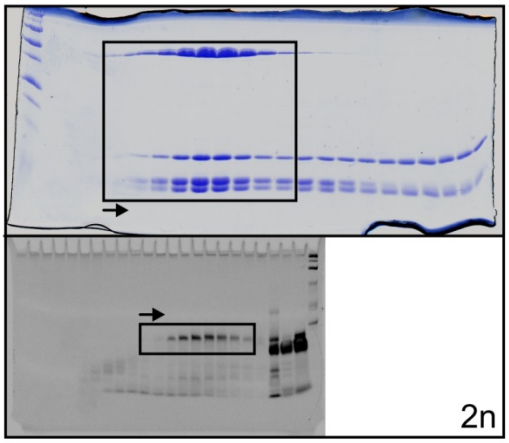

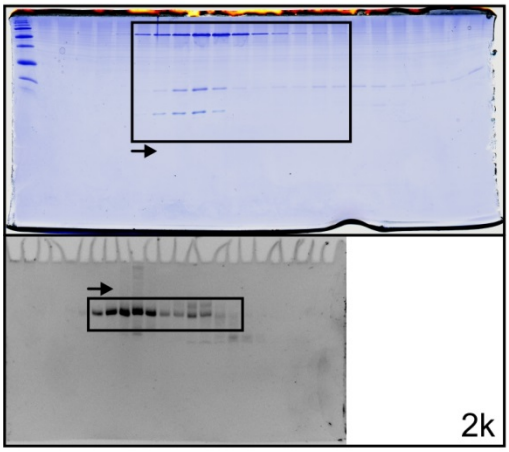

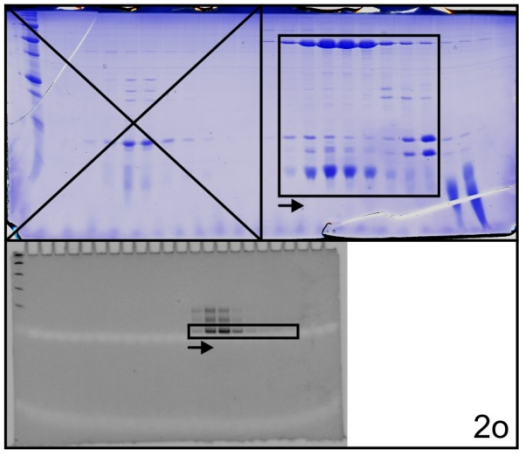

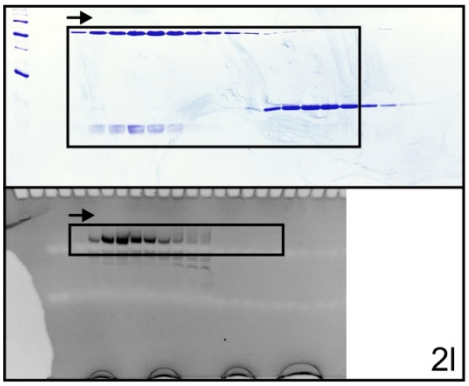

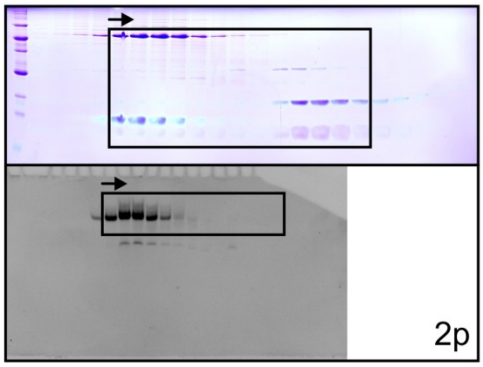

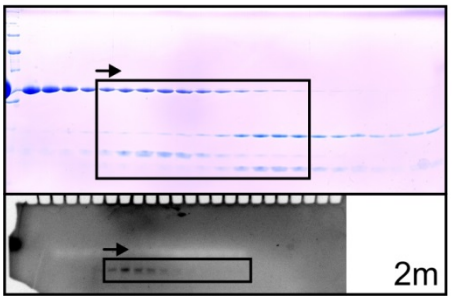

74

Original Scans, Figure 4

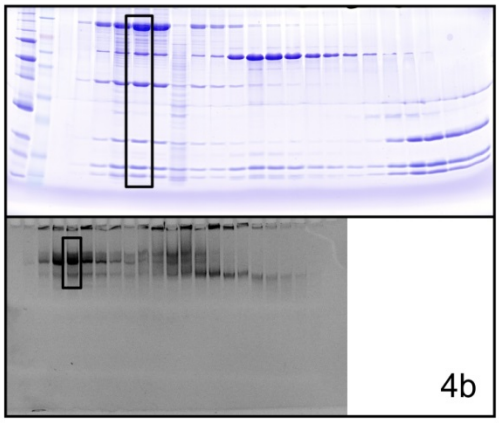

Original Scans, Figure 6

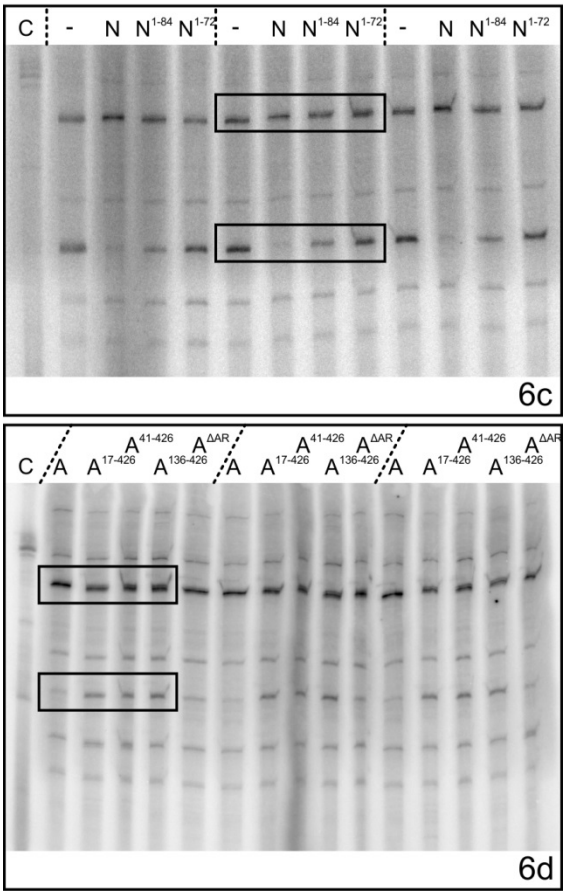

75

76

Supplementary Figure 2. Full scans of all gels shown in this work. Regions shown in the respective figures are boxed.

Supplementary Tables

Supplementary Table 1. Crystallographic data[a]

	λN^{1-84}-$NusA^{\Delta AR2}$-NusB-NusE-*nut* RNP	$NusA^{100-426}$
Data collection		
Wavelength [Å]	0.918	0.918
Temperature [K]	100	100
Space group	$P2_12_12_1$	$P2_1$
Unit cell parameters		
Axes [Å]	95.8, 101.8, 279.9	74.7, 147.2, 52.4
Angles [°]	90.0, 90.0, 90.0	90.0, 112.56, 90.0
Resolution [Å]	50-3.35 (3.55-3.35)	50-2.14 (2.27-2.14)
Reflections		
Unique	40077 (6372)	28443 (4469)
Completeness [%]	99.3 (98.3)	99.1 (96.5)
Redundancy	7.3 (7.5)	6.8 (6.7)
I/σ(I)	11.6 (0.9)	12.2 (1.1)
R_{meas}(I) [%]	16.1 (217.7)	11.7 (161.9)
$CC_{1/2}$ [%]	99.9 (64.1)	99.9 (97.2)
Refinement		
Resolution [Å]	39.52-3.35 (3.43-3.35)	46.94-2.14 (2.21-2.14)
Reflections		
Number	39986 (2665)	28428 (2563)
Completeness [%]	99.4 (98.9)	99.4 (95.0)
Test Set [%]	5.0 (5.0)	5.0 (5.0)
R_{work}	29.6 (46.5)	21.5 (36.5)
R_{free}	33.5 (49.6)	24.4 (37.1)
ESU[(b)] [Å]	0.62	0.37
Contents of A.U.[(c)]		
Protein (mol./res.)	8/1529	1/319
RNA (mol./res.)	2/56	-
Mean B factors [$Å^2$]		
Wilson	117.5	48.5
Protein	142.7	63.6
RNA	141.9	-
Water	-	58.0
Ramachandran plot[(d)]		
Favored [%]	92.9	99.1
Outliers [%]	0.1	0
Rmsd[(e)]		
Bond lengths [Å]	0.004	0.003
Bond angles [°]	0.845	0.638

[(a)] Values for highest resolution shell in parentheses.
[(b)] ESU – estimated overall coordinate error based on maximum likelihood.
[(c)] A.U. – asymmetric unit.
[(d)] Calculated with MolProbity[13].
[(e)] Rmsd – root-mean-square deviation from target geometry.

Supplementary Table 2. Chemical cross-linking-mass spectrometry (CX-MS) of a λN-NusA$^{\Delta AR2}$-NusB-NusE-*nut* RNP[a]

P1[b]	Residue	P2[b]	Residue	Cα-Cα (Å)	Reagent	Explanation[c]
NusA NTD	3	λN	77	13	BS3	
NusA NTD	4	λN	77	10	DMTMM	
NusA NTD	37	λN	77	31	BS3	
NusA NTD	57	λN	77	29	DMTMM	
NusA NTD-S1	111	λN	68	15	DMTMM	
NusA NTD-S1	111	λN	77	15	BS3	
NusA NTD-S1	132	λN	43	12	DMTMM	
NusA KH1	218	NusB	82	19	DMTMM	
NusA KH1	239	λN	45	23	BS3	
NusA KH1	243	NusB	76	15	DMTMM	
NusA KH2	335	λN	31	10	DMTMM	
NusA AR1	391	λN	77	88	DMTMM	λN$^{34-47}$-AR1
NusA AR1	411	λN	14	42	BS3	λN$^{34-47}$-AR1
NusA AR1	411	λN	68	74	DMTMM	λN$^{34-47}$-AR1
NusA AR1	422	λN	19	35	DMTMM	
NusA AR1	423	λN	19	37	DMTMM	λN$^{34-47}$-AR1
NusA AR1	423	λN	31	35	DMTMM	
NusA AR1	423	λN	68	67	DMTMM	λN$^{34-47}$-AR1
NusA AR1	423	λN	77	73	DMTMM	λN$^{34-47}$-AR1
NusE	27	λN	45	14	DMTMM	

(a) Cross-links between residues whose Cα atoms are between 35 and 45 Å apart in the λN$^{1-84}$-NusA$^{\Delta AR2}$-NusB-NusE-*nut* RNP crystal structure are colored yellow. Cross-links between residues whose Cα atoms are more than 45 Å apart in the λN$^{1-84}$-NusA$^{\Delta AR2}$-NusB-NusE-*nut* RNP crystal structure are colored red.

(b) P1/P2, first/second protein or protein domain of a cross-linked pair; NusA NTD-S1, NTD-S1 connector helix.

(c) Explanation for cross-links that show discrepancies to the crystal structure; λN$^{34-47}$-AR1, cross-link due to the alternative λN$^{34-47}$-NusA AR1complex.

Supplementary Table 3. Chemical cross-linking-mass spectrometry (CX-MS) of a λN-based transcription antitermination complex (TAC)[a]

[a] Cross-links between residues whose Cα atoms are between 35 and 45 Å apart in the cryo-EM model are colored yellow. Cross-links between residues whose Cα atoms are more than 45 Å apart in the cryo-EM model are colored red.
[b] P1/P2, first/second protein or protein domain of a cross-linked pair; NusA NTD-S1, NTD-S1 connector helix; NusA KH2-AR1, KH2-AR1 connector helix; NusG NTD-CTD, NTD-CTD linker.
[c] Explanation for cross-links that show discrepancies to the cryo-EM model; λN^{34-47}-AR1, cross-link due to the alternative λN^{34-47}-NusA AR1 complex; flex, cross-link involving residues that reside in highly flexible regions or in regions known to undergo conformational changes. Remaining discrepancies most likely originate from a minor fraction of aggregated material.

Supplementary Table 4. Chemical cross-linking-mass spectrometry (CX-MS) of a transcription elongation complex (TEC) lacking λN[a]

[a] Cross-links between residues whose Cα atoms are between 35 and 45 Å apart in the cryo-EM model of the TAC are colored yellow. Cross-links between residues whose Cα atoms are more than 45 Å apart in the cryo-EM model of the TAC are colored red. Cross-links differing between TAC and TEC (lacking λN) are highlighted in green.
[b] P1/P2, first/second protein or protein domain of a cross-linked pair; NusA NTD-S1, NTD-S1 connector helix; NusG NTD-CTD, NTD-CTD linker.
[c] Cα-Cα distances are from the TAC structure.

Supplementary References

1. Mooney, R. A. *et al.* Regulator Trafficking on Bacterial Transcription Units In Vivo. *Mol. Cell* **33**, 97-108, (2009).
2. Mogridge, J. *et al.* Independent ligand-induced folding of the RNA-binding domain and two functionally distinct antitermination regions in the phage lambda N protein. *Mol. Cell* **1**, 265-275, (1998).
3. Mah, T. F., Li, J., Davidson, A. R. & Greenblatt, J. Functional importance of regions in Escherichia coli elongation factor NusA that interact with RNA polymerase, the bacteriophage lambda N protein and RNA. *Mol. Microbiol.* **34**, 523-537, (1999).
4. Bonin, I. *et al.* Structural basis for the interaction of Escherichia coli NusA with protein N of phage lambda. *Proc. Natl. Acad. Sci. USA* **101**, 13762-13767, (2004).
5. Prasch, S. *et al.* Interaction of the intrinsically unstructured phage lambda N Protein with Escherichia coli NusA. *Biochemistry* **45**, 4542-4549, (2006).
6. Mishra, S., Mohan, S., Godavarthi, S. & Sen, R. The interaction surface of a bacterial transcription elongation factor required for complex formation with an antiterminator during transcription antitermination. *J. Biol. Chem.* **288**, 28089-28103, (2013).
7. Mah, T. F., Kuznedelov, K., Mushegian, A., Severinov, K. & Greenblatt, J. The alpha subunit of E. coli RNA polymerase activates RNA binding by NusA. *Genes Dev.* **14**, 2664-2675, (2000).
8. Schweimer, K. *et al.* NusA Interaction with the alpha Subunit of E-coli RNA Polymerase Is via the UP Element Site and Releases Autoinhibition. *Structure* **19**, 945-954, (2011).
9. Zhou, Y., Mah, T. F., Greenblatt, J. & Friedman, D. I. Evidence that the KH RNA-binding domains influence the action of the E. coli NusA protein. *J. Mol. Biol.* **318**, 1175-1188, (2002).
10. Rees, W. A., Weitzel, S. E., Yager, T. D., Das, A. & von Hippel, P. H. Bacteriophage lambda N protein alone can induce transcription antitermination in vitro. *Proc. Natl. Acad. Sci. USA* **93**, 342-346, (1996).
11. Burmann, B. M. *et al.* A NusE:NusG complex links transcription and translation. *Science* **328**, 501-504, (2010).
12. Strauss, M. *et al.* Transcription is regulated by NusA:NusG interaction. *Nucleic Acids Res.*, (2016).
13. Chen, V. B., Wedell, J. R., Wenger, R. K., Ulrich, E. L. & Markley, J. L. MolProbity for the masses-of data. *J Biomol NMR* **63**, 77-83, (2015).